NASA Technical Memorandum 85721

Evaluation of the Langley 4- by 7-Meter Tunnel for Propeller Noise Measurements

P. J. W. Block and Garl L. Gentry, Jr.

DECEMBER 1984

NASA

NASA Technical Memorandum 85721

Evaluation of the Langley 4- by 7-Meter Tunnel for Propeller Noise Measurements

P. J. W. Block and Garl L. Gentry, Jr.
Langley Research Center
Hampton, Virginia

National Aeronautics
and Space Administration

**Scientific and Technical
Information Branch**

1984

Contents

Summary

An experimental and theoretical evaluation of the Langley 4- by 7-Meter Tunnel was conducted to determine its suitability for obtaining propeller noise data. This report describes the tunnel circuit and open test section. An experimental evaluation is performed using microphones placed in and on the tunnel floor. The reflection characteristics and background noise are determined. The predicted source (propeller) near-field/far-field boundary is given using a first-principles method. The effect of the tunnel-floor boundary layer on the noise from the propeller is also predicted. A propeller test stand used for part of this evaluation is also described. The measured propeller performance characteristics are compared with those obtained at a larger scale, and the effect of the test-section configuration on the propeller performance is examined. Finally, propeller noise measurements were obtained on an eight-bladed SR-2 propeller operating at angles of attack of $-8°$, $0°$, and $4.6°$ to give an indication of attainable signal-to-noise ratios.

Introduction

In recent years, studies have shown that turboprop-powered aircraft may offer significant fuel savings over turbofan-powered aircraft (ref. 1). Thus, new aircraft propulsion systems are incorporating new and advanced propeller concepts such as highly swept and tapered blades, pusher configurations, and counter-rotation propellers. However, the noise impact of these propellers and the effect of their installation on the noise radiation is of concern from the cabin or interior noise standpoint as well as from the standpoint of the community. To assess the magnitude of the noise impact, near-field and far-field propeller noise measurements are needed on advanced propeller configurations. These measurements are used to validate available prediction methods and to supplement the data base on advanced propeller installation effects. There are few wind-tunnel or flow facilities which permit high-quality propeller noise data to be obtained over a wide range of test parameters. The Langley 4- by 7-Meter Tunnel, however, is attractive for making such measurements because of its large flow area, large open test section, and remote drive-fan location. Also, sound-absorbing materials may be applied to the open test section and removed with relative ease. In this report, the Langley 4- by 7-Meter Tunnel is evaluated for the purpose of making acoustic measurements on model scale propellers.

Several acoustic evaluations (refs. 2 and 3) have been conducted in the Langley 4- by 7-Meter Tunnel. (The Langley V/STOL Tunnel in ref. 3 has since been renamed the Langley 4- by 7-Meter Tunnel.) However, these evaluations were conducted with microphones mounted on support stands as opposed to microphones flush mounted in large surfaces such as the tunnel floor. The latter method is preferred because it eliminates the support-stand flow noise as well as the frequency dependence of the reflections from the tunnel floor. The disadvantage of a flush-mounted microphone is the effect of the boundary layer or velocity gradient over the surface in which the microphone is mounted (ref. 4). At low forward speeds (M = 0.1), it is anticipated that the effect on the sound propagation is small; however, a theoretical investigation is warranted on the basis of the source frequencies of interest.

This report gives a theoretical and experimental evaluation of the Langley 4- by 7-Meter Tunnel to determine its suitability for obtaining propeller noise data. The tunnel circuit and open test section, as well as a propeller test stand employed for part of this evaluation, are also described. An acoustic evaluation is performed using microphones placed in and on the tunnel floor. The reflection characteristics and background noise are determined. Analytical predictions are used to determine the source (propeller) near-field/far-field boundary at several angles to the axis using the first-principles method given in reference 5. The theoretical effect of the tunnel-floor boundary layer on the noise from the propeller is also predicted using the method described in reference 4. The measured propeller performance characteristics are compared with those obtained at a larger scale, and the effect of the test-section configuration on propeller performance is examined. Finally, propeller noise measurements were obtained on an eight-bladed SR-2 propeller operating at angles of attack of $-8°$, $0°$, and $4.6°$ to give an indication of attainable signal-to-noise ratios.

Symbols

Dimensional quantities are presented in both the International System of Units (SI) and U.S. Customary Units. Measurements and calculations were made in U.S. Customary Units.

C_P	power coefficient, $P/\rho n^3 d^5$
C_T	thrust coefficient, $T/\rho n^2 d^4$
d	propeller diameter
f	frequency
J	propeller advance ratio, U/nd
M	Mach number
n	number of revolutions per second
P	power absorbed by propeller
p	acoustic-pressure amplitude
q	free-stream dynamic pressure

R	observer distance
T	propeller thrust
U	tunnel velocity
u	magnitude of fluctuating component of tunnel velocity
x	streamwise dimension along tunnel floor
α	angle of attack or pitch angle of propeller axis with respect to airstream
$\beta_{.75}$	propeller pitch setting at 0.75 radial station with respect to plane of rotation
δ	boundary-layer thickness
ρ	air density

Abbreviations:

OTS	open test section
mic	microphone
OASPL	overall sound pressure level
SNR	signal-to-noise ratio
SPL	sound pressure level

Tunnel Description

Tunnel Circuit

The Langley 4- by 7-Meter Tunnel (formerly the Langley V/STOL Tunnel) is a closed single-return atmospheric wind tunnel with a speed range to 338 ft/sec (200 knots, 103 m/sec) and a unit tunnel Reynolds number to 2.1×10^6 per foot (6.89×10^6 per meter). An external view of the tunnel circuit is given in figure 1. A schematic of the major components is shown in figure 2. The tunnel circuit is described, beginning with the settling chamber, as follows. The settling chamber is approximately 57 ft (17 m) wide and 50 ft (15 m) high. During the test there were two turbulence screens in this section. Between the settling chamber and test section there is a 9 to 1 contraction ratio. The test section is 50 ft (15 m) long and permits closed-wall or open-wall operation. The closed-test-section dimensions are 21.75 ft (6.63 m) wide by 14.5 ft (4.42 m) high. (The open-test-section configuration employed in this experiment is described in the next section.) There are three diffusers and two corners with turning vanes between the test section and the tunnel drive fan which place the fan in the opposite leg of the tunnel from the test section. (See fig. 2.) This remote placement of the fan has advantages from an acoustic standpoint, because it provides the longest possible path length of the fan noise to the test section. The fan, which has nine blades and is 40 ft (12.2 m) in diameter, is powered by an ac motor and a dc motor, which are housed in the nacelle. Together they provide 8000 hp (5970 kW) to drive the fan over a variable speed range from 0 to 275 rpm. The fan section is followed by another diffuser section which transitions into the settling chamber around two more corners.

Test-Section Configurations

The Langley 4- by 7-Meter Tunnel can have many test-section configurations. The two standard configurations are closed (ceiling and both sidewalls are down) and open (ceiling and both sidewalls are up). In the open test section (OTS), the ceiling is 24.5 ft (7.5 m) above the floor. The sidewalls also retract to that height. In certain ranges of tunnel speed, a flow pulsation existed which required the addition of triangular tabs to the tunnel exit. Thus the OTS with tabs constitutes another configuration of interest for acoustic testing.

Open Test Section

Description. A plan view of the open test section (OTS) is given in figure 3. At the end of the contraction (labeled station 0) the flow exits through a rectangular nozzle 21.75 ft (6.63 m) wide and 14.5 ft (4.42 m) high into a test chamber which is approximately 80 ft (24.4 m) long, 60 ft (18.3 m) wide, and 32 ft (9.75 m) high. The floor was not removed for the test. There are two test bays which are indicated by the large circles in figure 3. The rear bay was used in this test. The straight sting-support post was located at station 40 ft (12.2 m), which placed the model at approximately 28 ft (8.53 m) from the nozzle exit. (See fig. 2, side view.) The flow exited the test chamber through a large bell-mouthed collector into the first diffuser at station 68 ft (20.73 m). Figure 4 is a photograph of the propeller and bell-mouthed collector of the open test section.

The maximum velocity in the open test section is restricted to about 338 ft/sec (200 knots, 103 m/sec).

Flow quality. In the open test section, the flow is uniform with turbulence intensities from 2 to 8 percent. The effect of turbulence on propeller noise is a subject of study in and of itself; however, there is no evidence that this level has a measurable effect on the first few harmonics of the propeller noise. Tunnel speeds corresponding to $q = 11$ and 20 were selected because they represented the conditions with the lowest turbulence intensity (2 percent).

Propeller Test Setup

Propeller

The propeller was an eight-bladed aluminum SR-2 design, 16.9 in. (0.429 m) in diameter. (See fig. 4.) The

planform and twist distribution for the SR-2 propeller are documented in reference 6. It was fabricated on a numerically controlled milling machine to a tolerance of ±0.003 in. (0.076 mm) on the airfoil contour and ±0.005 in. (0.127 mm) on span warpage. When placed in the hub, the radial-position tolerance was ±0.0025 in. (0.064 mm). The hub permitted nominal blade pitch-angle settings from −2° to 60° in 1° increments through a collective pitch gear. The propeller blades were pinched or clamped into the hub such that when assembled the blades did not wobble. The spinner, hub, and blades were dynamically balanced not to exceed 0.01 oz-in. (7.06×10^{-5} N-m) of imbalance. The propeller rotated clockwise looking upstream.

Nacelle, Sting, and Balances

The nacelle was a body of revolution with a maximum outside diameter (fig. 5) of 6 in. (0.152 m). It housed a 29-hp (21.6-kW) 10 000-rpm water-cooled electric motor and two balances. However, of these balances, the four-component and thrust and torque balances were not used in this test. Instead, the six-component balance located in the sting was used for all force measurements.

The nacelle was attached to a straight sting through the six-component balance and an aerodynamic fairing. The sting height and pitch were adjustable. Propeller heights of 3 ft (0.914 m) and 6 ft (1.829 m) were used. A pitch range from −8° to 4.6° was possible if the height of the propeller axis were fixed at 3 ft (0.914 m) above the floor.

The repeatability of the force data was checked for several conditions and found to be on the order of 0.02 for C_T and 0.03 for C_P. The size of the data symbols (performance data) reflects the magnitude of this uncertainty.

Acoustic Measurements

To eliminate the effects of the reflections from the tunnel floor, which, in this facility is the closest reflecting surface to the model, the microphones were flush mounted in the tunnel floor. This measurement scheme was a precursor to a moveable microphone carriage scheme which would operate 2 ft above the tunnel floor and support flush-mounted microphones. Theoretically, microphones that are flush mounted in a large surface record a pressure doubling. With flush microphone mounting, the free-field acoustic levels have been shown to be reliably obtained from the measured signal over the frequency and incident-angle range of interest (ref. 7). The velocity gradient produced by the surface and the introduction of extraneous noise from the floor vibration are addressed subsequently.

Microphone Mounting Description

Figure 6 is a photograph of the microphone mount in the tunnel floor. The Langley 4- by 7-Meter Tunnel floor is comprised of 1/4-in. (6.35-mm) and 3/8-in. (9.52-mm) thick braced steel plates. A 3/4-in. (19.05-mm) hole was drilled in these plates to provide a clearance hole for the 1/2-in. (12.7-mm) condenser-type microphone. A vibration damper made from 1-in. (25.4-mm) thick rubber-sponge sheeting was glued to the underside of the tunnel floor. Next a 1-in. (25.4-mm) thick piece of steel bar stock 5 in. (0.127 m) in diameter was glued to the rubber sponge to provide a damping weight for the microphone. The microphone was inserted through the steel bar stock, rubber sponge and tunnel floor, and was secured in place by setscrews in the steel bar stock. This mounting procedure was used in an attempt to minimize the effect of the tunnel floor vibrations on the microphone signals. Accelerometers attached to the bar stock verified that, during the tunnel operation, the microphone was not subjected to measurable vibration levels over the frequency range of interest ($f > 80$ Hz). Therefore, it was concluded that the tunnel floor vibration presented no serious contamination of the acoustic signal.

Microphone Locations

Eight microphones were used during the course of the test program. Their locations are shown by the numbered circles in figure 7. Microphones 1 through 5 were mounted in the floor as described previously with microphone 1 placed directly under the propeller or source. These five were used for measuring the propeller noise. At the 3-ft (0.91-m) height microphone 1 was located 2.1 propeller diameters from the propeller axis. Microphones 2 through 5 were 5.7 diameters from the axis. At these distances the microphones are usually considered to be in the far field of the propeller. Although no tests were done to confirm this, a first-principles prediction method is used to identify the beginning location of the far field. These results are given in the section "Results." Microphones 6, 7, and 8 were simply placed on the concrete floor (no support stands), 8 ft (2.4 m) from the tunnel surfaces which were expected to cause contaminating reflections. Microphones 6, 7, and 8 were used only during the acoustic evaluation to determine the reflection characteristics of the sidewall, bell-mouthed collector, and control room, respectively.

Test Conditions

Setup for Acoustic Evaluation of Open Test Section

Measurements. To determine the potential for contamination from the various reflecting surfaces, such

as the walls and ceiling of the open test section, a "tone-burst" procedure was employed. A high-power precision speaker was suspended from the nacelle and positioned to the location that the propeller would occupy, which was initially 6 ft (1.83 m) above the floor. The speaker was fitted with a conical horn 7.5 in. (0.191 m) in length and 7 in. (0.178 m) in diameter at the mouth. The signal generated by the speaker contained a tone burst of from 2 to 8 cycles of a specified frequency. These bursts were spaced or separated in time nominally by one-half second. This spacing permitted each microphone to record the first burst amplitude and to receive the reflected signals from the various surfaces in the open test section. The number of cycles per burst was varied so that the reflected pulse from each surface could be identified. A typical example of the output from this evaluation is shown in figure 8. In the figure the reflected amplitudes from several surfaces are identified using the distance of the microphone and sound source from the surface as well as the sound speed. This evaluation covered the frequency range from 300 Hz to 5 kHz at the following frequencies: 300, 500, 750, 1000, 1250, 2000, 2500, 3000, 3500, 4000, and 5000 Hz. For the evaluation of the OTS surface reflection characteristics, the tunnel was operated with wind off only.

For the evaluation of the OTS background noise characteristics at the floor-mounted microphone positions, tunnel speeds of 105 ft/sec (32 m/sec) and 142 ft/sec (43.3 m/sec) were chosen. These correspond to velocities where the turbulence intensity was the lowest (2 percent). Also, for this part of the study, the propeller spinner and nacelle were present, but the blades were removed and the holes in the spinner were taped.

Predictions. Theoretical methods were also employed where experimental data were lacking. The predicted near-field/far-field boundary was estimated using a first-principles linear-noise source model for the propeller (ref. 5). The SR-2 propeller operating at $\beta_{.75} = 12.6°$ and $J = 0.423$ was used as the source. The noise at observer distances of 1 to 4.5 propeller diameters d were calculated in $0.5d$ steps. This calculation was done at three angles—in-plane (0°) and at 30° and 60° in front of the disk plane.

This same source was used to determine the magnitude of the effect of the boundary layer at frequencies associated with model propellers. The source (propeller) was placed 3 ft (0.914 m) above the floor. A forward velocity of 100 ft/sec (30.5 m/sec) was used with boundary-layer thicknesses δ of 0.125 in. (0.318 cm), 0.5 in. (1.27 cm), 2 in. (5.08 cm), and 4 in. (10.16 cm). The tunnel is estimated to have a 4-in-thick boundary layer. A moveable microphone carriage is estimated to have a boundary-layer thickness less than 0.125 in.

Propeller Performance

An available performance data set on a larger eight-bladed SR-2 propeller ($d = 24.5$ in. (0.622 m)) guided the test conditions for the propeller performance tests. For comparison purposes, these conditions were duplicated in terms of the blade angle ($\beta_{.75}$ nominally 30° and 42°), the forward velocity ($U = 105$ ft/sec (32 m/sec)), and the range of advance ratio ($J = 0.8$ to 1.8).

To investigate whether the test-section configuration has an effect on propeller performance, one propeller blade angle was used ($\beta_{.75} = 30.5°$). The three test-section configurations were (1) closed, (2) open with tabs, and (3) open without tabs. This investigation was conducted at three forward speeds corresponding to tunnel free-stream dynamic pressures of 4.5, 18.0, and 28.3 lb/ft^2 (215, 862, 1355 Pa).

Propeller Noise

The test conditions for the propeller noise measurements are given in table 1. Only one blade angle was used ($\beta_{.75} = 30.5°$). Two forward speeds (105 ft/sec (32 m/sec) and 142 ft/sec (43.3 m/sec)) were examined at three propeller pitch angles (−8°, 0°, and 4.6°). The rotational speed for all the tests was fixed at 10 000 rpm.

Results

Acoustic Evaluation—Measurements

Surface reflections. The results of the tone-burst evaluation are given in decibels as

$$\text{Reflected amplitude ratio} = 20 \log_{10} \left(\frac{\text{Peak reflected amplitude}}{\text{Peak incident amplitude}} \right)$$

and can be summarized as follows. For microphones 1 through 5, reflections from the raised tunnel ceiling arrived at a level from 16 to 20 dB below the initial-incident (first received) signal and were independent of frequency. This large reduction of the reflected amplitude is attributed to the large path difference of 34 to 37 ft (10.4 to 11.3 m). The direct path was 6 ft (1.83 m). Similarly, reflections from the tunnel sidewall arrived from 15 to 22 dB below the first received signal. The sidewall path-length difference for microphone 1 was 46 ft (14.0 m). The reflections from the bell-mouthed collector appeared to be stronger arriving at levels from 9 to 16 dB below the initial-incident signal level. These levels, however, may have resulted from a double reflection from the sidewall and the circular collector. (See fig. 7.) These signals would have arrived with almost no time separation between them. For this test setup, however, microphones 1 through 5

received the strongest reflections from the sting support post. (See figs. 7 and 8.) Fortunately, because of the relatively small diameter of the sting support post (1.5 ft, 0.46 m), these reflections only appeared to be noticeable at frequencies above 2000 Hz. Reflections at these higher frequencies are easily treated by the application of open-cell acoustic foam. These results indicate that the data from the microphones which were used for propeller noise measurements were not affected by tunnel wall reflections at a distance corresponding to 4.2 propeller diameters. As the source is moved closer to the microphones, the reflected amplitude ratio given in this section becomes much smaller. For near-field measurements where distances are less than two propeller diameters, the ratio is smaller. Therefore, the reflected amplitudes are even smaller. This evaluation was done without any acoustic treatment in the OTS. It is anticipated that these ratios could be further improved with the application of acoustic foam to the walls and ceiling. It is also anticipated that the low reflected-amplitude ratios, coupled with the presence of the flow field during tunnel operation, would hinder the formation of standing waves in the OTS.

Turning to the reflection characteristics of the walls themselves, the results from the sidewall (mic 6), collector (mic 7), and control-room (mic 8) evaluation are shown in figure 9. The three surfaces are most reflective in the 1500- to 5000-Hz frequency range. In particular, the sidewall (mic 6) reflected almost 100 percent of the incident sound amplitude between 2500 and 3500 Hz. Therefore, acoustic data from microphones placed in the vicinity of 8 ft (2.4 m) from the sidewall are most seriously contaminated if the noise source of interest contains the major part of its energy in this frequency range. Below 1000 Hz, the reflected amplitudes are nominally 8 dB below the incident amplitude.

For the propeller noise tests, an open-cell acoustic-foam bat 6 in. (0.152 m) thick and equal in width to the diameter of the sting support post was applied to the sting support post. This post presented the only serious reflecting surface which could potentially affect the data obtained at microphone positions 1 through 5. (See fig. 8.) Foam bats were also applied to the sidewall and control room as a precautionary measure, because these surfaces would receive the largest amount of noise from the propeller and were the easiest to treat.

Background noise. Narrow-band pressure spectra of the tunnel background noise at tunnel speeds of 105 and 142 ft/sec (32 and 43 m/sec) are shown in figure 10. These data have not been corrected for pressure doubling. The analysis bandwidth is 19.5 Hz.

The absolute one-third-octave band levels of the background noise (streamlined nacelle without propeller) at free-stream dynamic pressures of 11 and 20 lb/ft^2 (527 and 958 Pa) are shown in figure 11. Data are not corrected for pressure doubling and have been high-pass filtered at 80 Hz. For this test condition, data above about 2000 Hz are influenced by the electronic noise floor of the recording instrumentation. Data between these frequencies (80 to 2000 Hz) are used to determine the acoustic source characteristics of the background noise in the OTS.

Normalization of the one-third-octave levels in figure 11 revealed that the two spectra collapse in the 100- to 400-Hz bands assuming a U^4 dependence of the noise on tunnel velocity. Data from 800 to 2000 Hz collapse assuming a U^6 dependence. This lower-frequency data collapse on U^4 indicates that the large-amplitude low-frequency ($f < 400$ Hz) noise is being produced by a fluctuating mass addition to (and removal from) the test chamber. That is, the flow has a fluctuating component either at the jet or at the exhaust from the OTS. The sound-pressure amplitude of a fluctuating mass-addition source is proportional to ρu^2 where ρ is the air density and u is the magnitude of the velocity fluctuations in the exit plane of the jet (end of the contraction) or of the exhaust (bell-mouthed collector). This mass-addition type of flow source is the most efficient radiator of sound (ref. 8). Thus, reducing the velocity fluctuations in these planes reduces this U^4 noise source accordingly.

The other identifiable noise source which is 3 to 4 dB lower in amplitude than the U^4 source is dominant in the 800- to 2000-Hz range. The dependence of this source on the sixth power of velocity indicates that the source is related to a fluid surface boundary. In particular, this U^6 noise source arises where the fluid separates from and attaches to a surface. In the OTS, the separation and attachment occur at the jet exit and at the bell-mouthed collector. The most likely candidate in the Langley 4- by 7-Meter Tunnel for producing most of this noise throughout the OTS is the jet exit because of the higher velocity shear. In wind tunnels where the airflow is controlled by surfaces and where removal of these surfaces is not an option, attenuation near or at the source may be considered for reducing the amount of acoustic energy reverberating throughout the open test section. The application of sound-absorbing foam near the source could serve to absorb some of this noise.

Acoustic Evaluation—Predictions

Near-field/far-field boundary. The far field is defined as that region of space where all the noise energy is radiant, travelling away from the source at the speed of sound. The acoustic pressure in this region decreases at a rate of 6 dB for every doubling of distance. The results from the theoretical study are given in figure 12.

The test conditions for this study were given previously. In figure 12, the predicted acoustic level (normalized by the predicted level at the closest observer position) is plotted against observer distance R (normalized by the propeller diameter) for three angles with respect to the propeller disk plane. The expected decrease in level for every doubling of distance is observed after about two propeller diameters in the in-plane direction and 30° direction and after about three propeller diameters in the 60° direction. For the tests described herein, microphone 1 is located at the very beginning of the far-field, and the other 4 microphones can be considered as safely in the far-field.

Effect of tunnel boundary layer. The predicted effect of the boundary layer on the noise measured beneath it is given in figure 13 for the first two harmonics of the propeller noise. Plotted against axial distance, x (streamwise direction) is the difference between the SPL with a boundary layer and the SPL without a boundary layer ($\delta = 0$). In this figure, $x = 0$ is directly under the propeller disk. The predictions indicate that in a small region where the sound waves arrive almost normal to the floor (-1 ft $< x <$ 1 ft (0.305 m)) there is an amplification of the acoustic signal level. This amplification is attributed to a focusing of the refracted rays as they are continuously turned in the boundary layer above the floor. For a 4-in. (10.16-cm) thick boundary layer, there is a predicted amplification of 2 dB. As expected, as the boundary-layer thickness δ decreases, the amplification decreases. Outside this amplification region (-1 ft $< x <$ 1 ft) there is an attenuation of the acoustic signal level. This attenuation is predicted to be as much as 10 dB for the second harmonic passing through a 4-in. boundary layer. The attenuation is attributed to the effects of convection and to refraction of the acoustic waves. As δ decreases to 0.125 in. (0.318 cm), the refraction and convection effects are reduced to within experimental measurement accuracy.

Propeller Performance

Comparison with larger scale. Performance data on a larger eight-bladed SR-2 propeller were obtained by George L. Stefko of the NASA Lewis Research Center. Reference 9 describes the test but does not include the data presented herein. To confirm the blade construction and performance results, two of the Lewis cases were duplicated in terms of the blade angle $\beta_{.75}$, the tunnel velocity U, and the advance ratio J. The performance comparisons are shown in figure 14, and good agreement is shown in both C_T and C_P.

Effect of test-section configuration. Figure 15 is a comparison of propeller performance for the three test-section configurations at three test-section dynamic pressures. The results show that for negative values of C_T and C_P the OTS with tabs consistently gives slightly lower values of the coefficients than the other two test-section configurations. However, this result may reflect the effect of the tabs, and not the propeller itself on the tunnel-velocity measurement.

Since the noise measurements were made at positive propeller thrust, where all configurations give the same results, the test-section configuration can be said to have no effect on performance.

Propeller Noise

The microphones mounted in the tunnel floor did not all detect the propeller noise at all test conditions at the initial propeller height of 6 ft (1.83 m) above the tunnel floor. When lowered to a height of 3 ft (0.91 m), however, the first two harmonics of propeller noise were usually detected or became visible above the background noise using on-line narrow-band analysis. (The on-line narrow-band analysis employed ensemble averaging to detect narrow-band signals in the random background noise.) For the test conditions reported herein, the signal-to-noise ratios (SNR) of the first harmonic (fundamental frequency) and second harmonic are presented and are considered representative of the overall sound pressure level (OASPL), since the second harmonic is typically 15 dB below the first. Also, all noise data presented were obtained at the 3-ft height.

In this initial test, an indication of the change of propeller noise radiation with angle of attack was investigated by rotating the propeller disk to fixed pitch angles of $-8°$, $0°$, and $4.6°$. Figure 16 is a typical narrow-band analysis. These results were obtained from microphone 1. The SR-2 propeller pitch setting was 30°, and the tunnel free-stream dynamic pressure was 11 lb/ft^2 (527 Pa). The data have not been corrected for pressure doubling.

The test conditions are in table 1 and the results are in tables 2 and 3 in terms of the SNR of the first two harmonics. That is,

$$\text{SNR} = \text{Level of signal harmonic} - \text{Level of background noise at corresponding frequency}$$

The level of the background noise is the level at the base of the spike representing the propeller harmonics. (See fig. 16.) The values in table 2 show that for the majority of conditions in the test matrix, the SNR of the fundamental frequency exceeded 20 dB, and all the SNR measurements exceeded 10 dB. The second harmonic (table 3) was typically 15 dB below the first and in some cases was not clearly detected above the tunnel background noise using on-line narrow-band analysis.

Here the propeller is relatively lightly loaded, and consequently the harmonic levels fall off rapidly.

In other cases, with higher levels of the higher harmonics generated (such as pusher configurations and counter-rotating propellers), more of the harmonics are expected to be visible above the tunnel background noise, because the tunnel noise levels decrease with increasing frequency.

Concluding Remarks

Conclusions from the initial evaluation of the Langley 4- by 7-Meter Tunnel for propeller noise measurements are summarized in the following paragraphs.

For the source locations and floor microphone installation employed herein, reflections from untreated open-test-section (OTS) surfaces arrived at levels typically 15 to 20 dB below the initial signal level. (The application of acoustic treatment and reducing the source-to-microphone distance are expected to improve these ratios considerably.) Thus, the OTS wall reflections pose no serious contamination potential for the measurement technique employed herein. It is also anticipated that the low reflected amplitude ratios coupled with the presence of the flow field during tunnel operation, would hinder the formation of standing waves in the OTS. The floor-mounted microphone signals were not contaminated by floor vibrations.

Microphones placed far from the propeller near untreated reflecting surfaces ((≈ 8 ft) (2.44 m)) experienced serious contamination.

Analysis of background noise measurements indicated that the large-amplitude low-frequency (100 to 400 Hz) noise was being produced by an unsteady flow supply to the test section. Another identifiable source (800 Hz to 2000 Hz) was related to the nozzle lip edge and collector flow-attachment region.

A theoretical study of the boundary-layer effects over a range of boundary-layer thicknesses indicated that a 4-in. (10.16-cm) tunnel-floor boundary layer had maximum amplification and attenuation effects of 2 and 10 dB, respectively, at a tunnel speed of 100 ft/sec (30.48 m/sec). These effects reduce to within the microphone measuring accuracy for a boundary layer thickness of 0.125 in. (0.318 cm).

Propeller performance data showed good agreement with those obtained elsewhere on the same propeller design.

The test-section configuration showed no measurable effects on propeller performance over positive thrust conditions.

For this size propeller (16.9-in. (42.93-cm) diameter) with an electric motor (29 hp (21.6 kW) at 10 000 rpm) for distances less than 5.7 diameters from the propeller axis, the signal-to-noise ratio (SNR) for the fundamental frequency exceeded 20 dB for most of the test matrix and was never lower than 10 dB. The SNR of the higher harmonics depended on the propeller operating condition. It is anticipated that pusher propellers and counter-rotation propellers will generate higher levels in the higher harmonics. Because the tunnel noise decreases with increasing frequency, acceptable signal-to-noise ratios are expected.

It is concluded from this study that high-quality near-field and far-field propeller noise data can be obtained in the Langley 4- by 7-Meter Tunnel using a flush-mounted microphone scheme of the type described herein.

Langley Research Center
National Aeronautics and Space Administration
Hampton, VA 23665
September 25, 1984

References

1. Mitchell, Glenn A.; and Mikkelson, Daniel C.: *Summary and Recent Results From the NASA Advanced High-Speed Propeller Research Program.* NASA TM-82891, [1982].
2. Hayden, R. E.; and Wilby, J. F.: *Sources, Path, and Concepts for Reduction of Noise in the Test Section of the NASA Langley 4- × 7-m Wind Tunnel.* NASA CR-172446-1, 1984.
3. Vér, István L.: *Acoustical Evaluation of the NASA Langley V/STOL Wind Tunnel.* NASA CR-145087, [1977].
4. McAninch, G. L.; and Rawls, J. W., Jr.: Effects of Boundary Layer Refraction and Fuselage Scattering on Fuselage Surface Noise From Advanced Turboprop Propellers. AIAA-84-0249, Jan. 1984.
5. Farassat, F.; and Succi, G. P.: The Prediction of Helicopter Rotor Discrete Frequency Noise. *Vertica*, vol. 7, no. 4, 1983, pp. 309–320.
6. Jeracki, Robert J.; Mikkelson, Daniel C.; and Blaha, Bernard J.: *Wind Tunnel Performance of Four Energy Efficient Propellers Designed for Mach 0.8 Cruise.* NASA TM-79124, 1979.
7. Willshire, William L., Jr.; and Nystrom, Paul A.: *Investigation of Effects of Microphone Position and Orientation on Near-Ground Noise Measurements.* NASA TP-2004, 1982.
8. Morse, Philip M.; and Ingard, K. Uno: *Theoretical Acoustics.* McGraw-Hill Book Co., Inc., c.1968.
9. Stefko, George L.; Bober, Lawrence J.; and Neumann, Harvey E.: *New Test Techniques and Analytical Procedures for Understanding the Behavior of Advanced Propellers.* NASA TM-83360, [1983].

TABLE 1. TEST CONDITIONS FOR PROPELLER NOISE MEASUREMENTS

Run	Tunnel		Propeller					
	q, lb/ft^2 (Pa)	U, ft/sec (m/sec)	$\beta_{.75}$, deg	α, deg	rpm	Thrust, lbf (N)	J, U/nd	C_T
3	11	105	30.5	−8.0	10 000	62.7 (279)	0.448	0.248
2	(527)	(32.0)		0.0		61.0 (271)		.241
6				4.6		59.5 (265)		.235
5	20	142	30.5	−8.0	10 000	44.9 (200)	0.605	0.183
4	(958)	(43.3)		0.0		42.4 (189)		.173
7				4.6		39.5 (176)		.161

TABLE 2. FIRST-HARMONIC SIGNAL-TO-NOISE RATIOS[1] FOR SR-2 PROPELLER AT ANGLE OF ATTACK

Tunnel		Propeller			SNR of first harmonic, dB				
q, lb/ft^2 (Pa)	U, ft/sec	rpm	Nominal thrust, lbf (N)	α, deg	Mic 1	Mic 2	Mic 3	Mic 4	Mic 5
11 (527)	105 (32.0)	10 000	61.0 (271)	−8.0	31.5	26.0	17.0	31.0	30.5
				0.0	36.5	22.5	22.0	29.0	26.0
				4.6	38.0	20.0	25.0	20.0	20.5
20 (958)	142 (43.3)	10 000	42.0 (187)	−8.0	23.0	15.0	10.5	20.0	22.0
				0.0	29.0	10.5	13.5	21.0	19.5
				4.6	29.5	14.0	14.0	19.0	15.5

[1]SNR = Signal level − Background noise level.

TABLE 3. SECOND-HARMONIC SIGNAL-TO-NOISE RATIOS[1] FOR SR-2 PROPELLER AT ANGLE OF ATTACK

Tunnel		Propeller			SNR of second harmonic, dB				
q, lb/ft^2 (Pa)	U, ft/sec	rpm	Nominal thrust, lbf (N)	α, deg	Mic 1	Mic 2	Mic 3	Mic 4	Mic 5
11 (527)	105 (32.0)	10 000	61.0 (271)	−8.0	9.5	7.0	3.5	7.0	10.0
				0.0	20.0	7.0	3.5	4.5	7.0
				4.6	21.5	4.5	6.0	3.0	6.0
20 (958)	142 (43.3)	10 000	42.0 (187)	−8.0	8.0	1.0	1.0	1.0	4.0
				0.0	16.5	2.0			3.0
				4.6	20.0	2.5	3.0	1.0	

[1]SNR = Signal level − Background noise level.

L-84-133

Figure 1. Langley 4- by 7-Meter Tunnel.

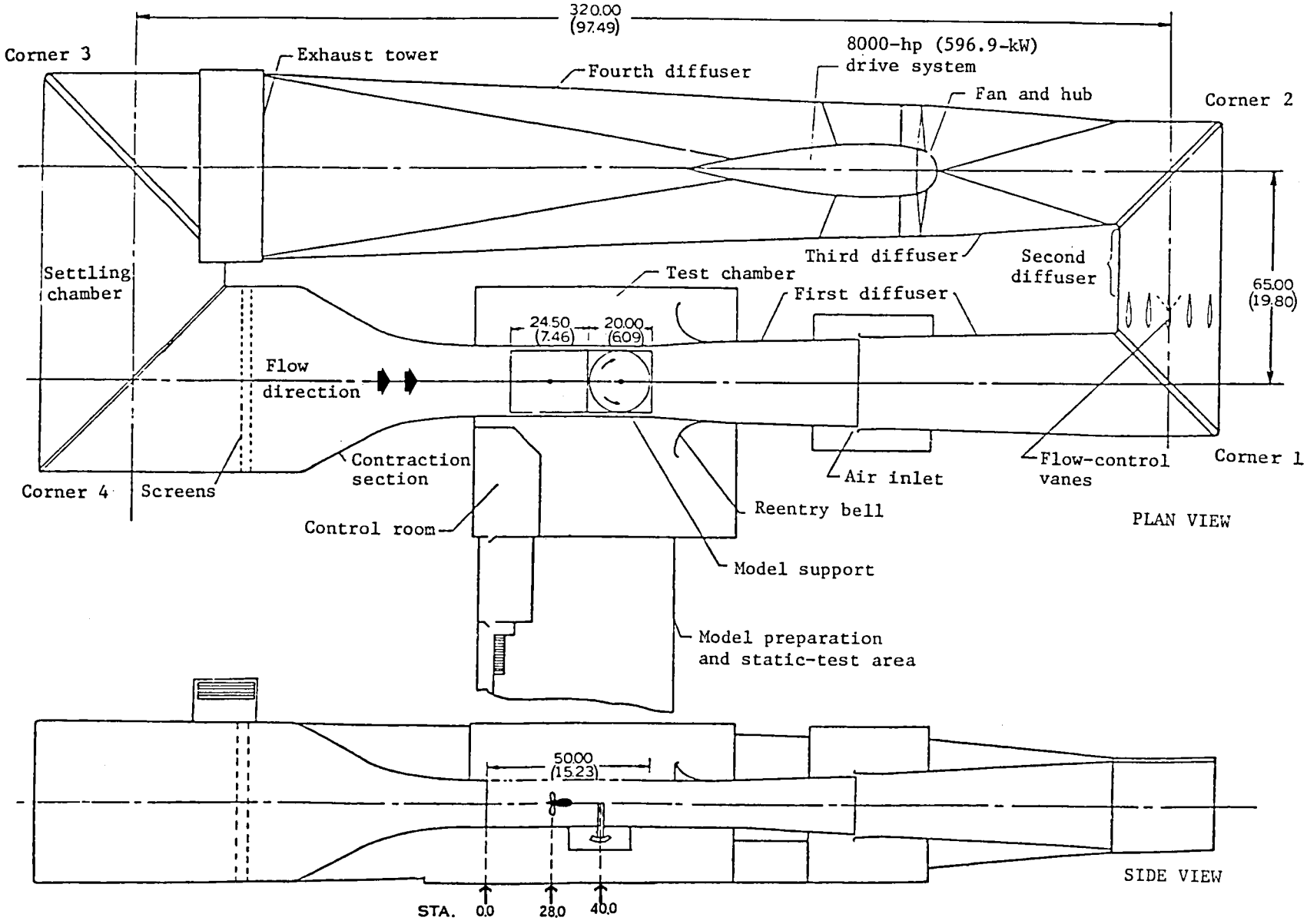

Figure 2. Schematic of Langley 4- by 7-Meter Tunnel. Dimensions are in ft (m).

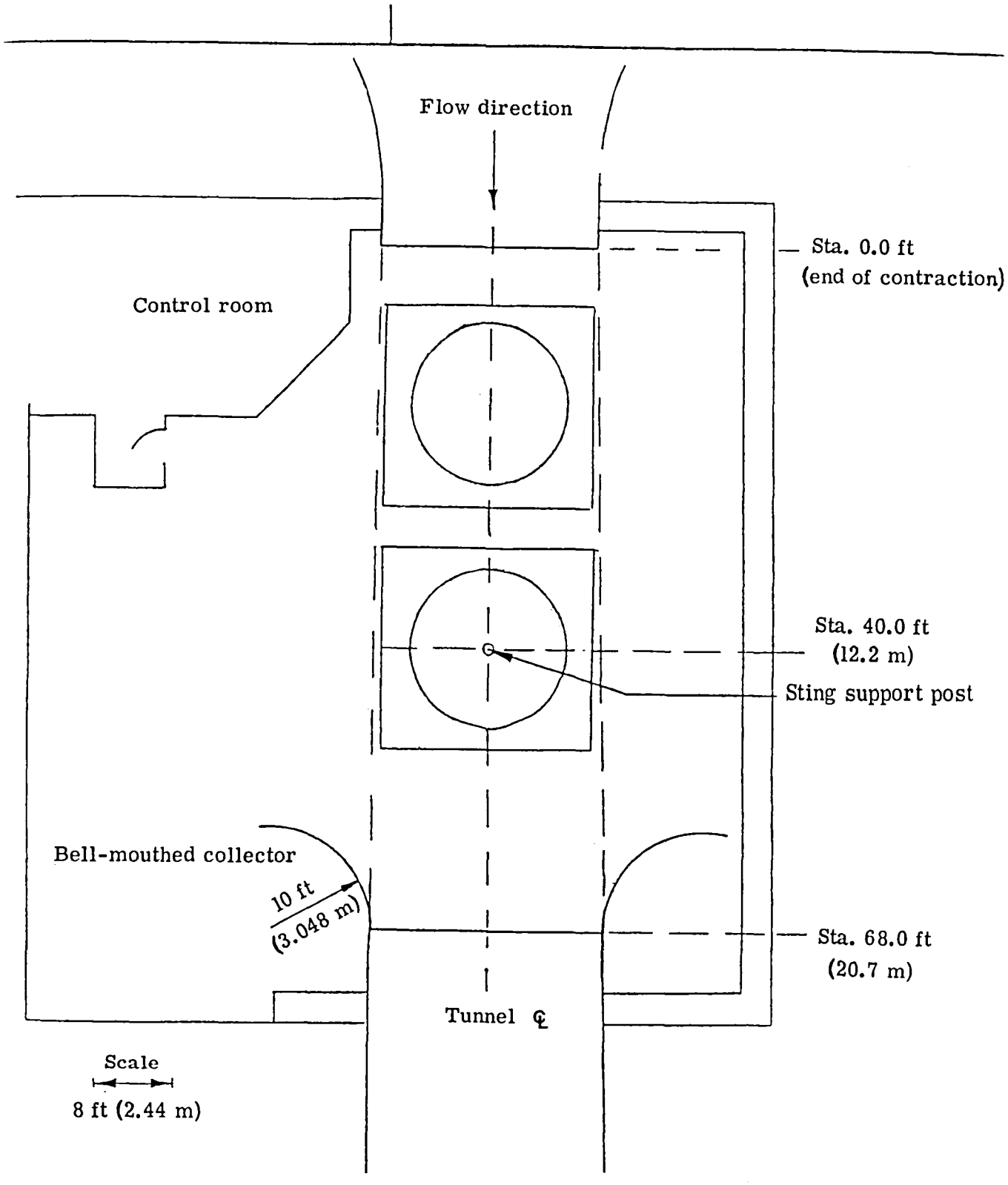

Figure 3. Plan view of open test section of Langley 4- by 7-Meter Tunnel.

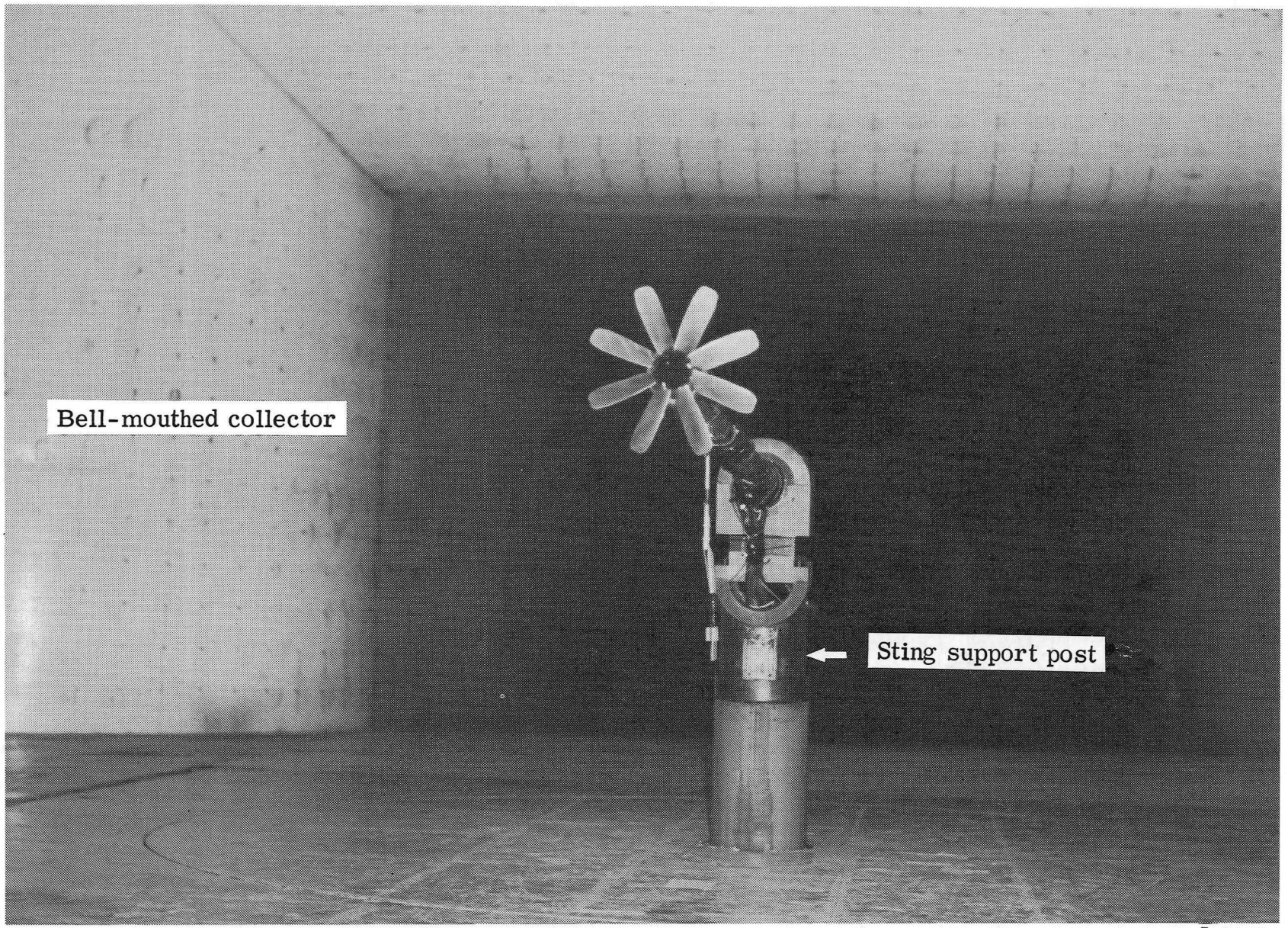

L-84-134

Figure 4. Langley 4- by 7-Meter Tunnel open test section looking downstream at bell-mouthed collector.

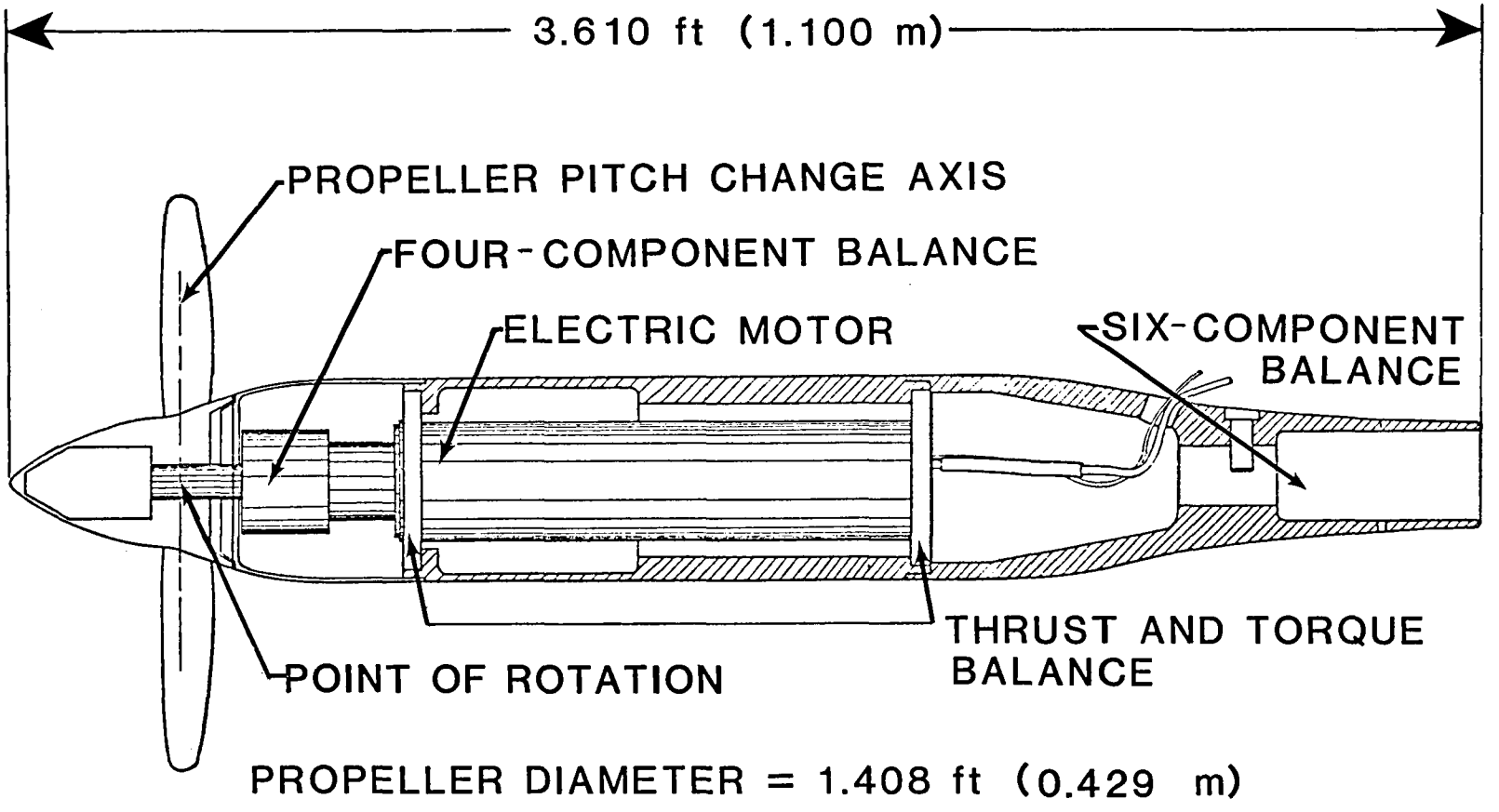

Figure 5. Schematic of nacelle.

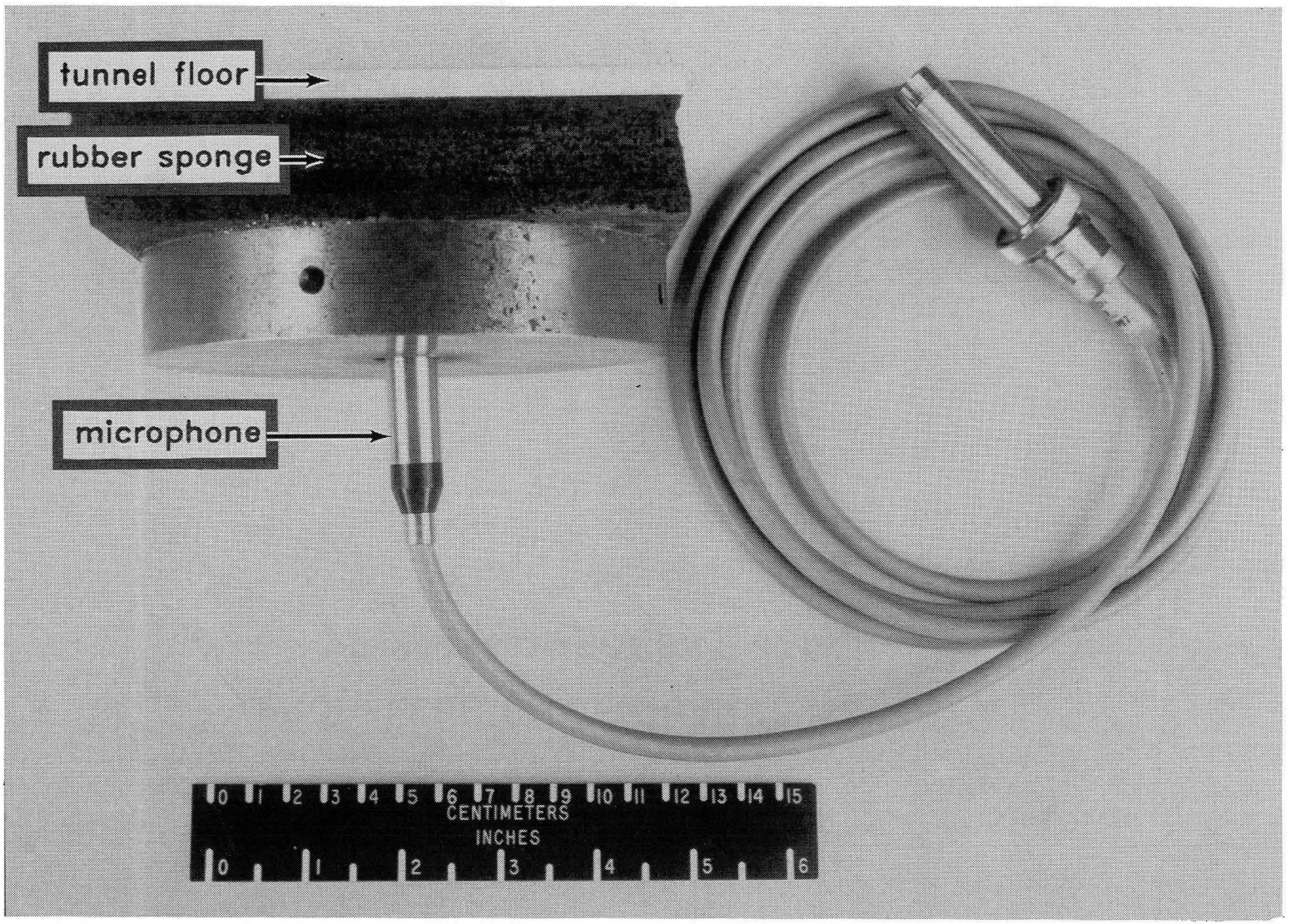

L-84-135

Figure 6. Microphone mount in floor of Langley 4- by 7-Meter Tunnel.

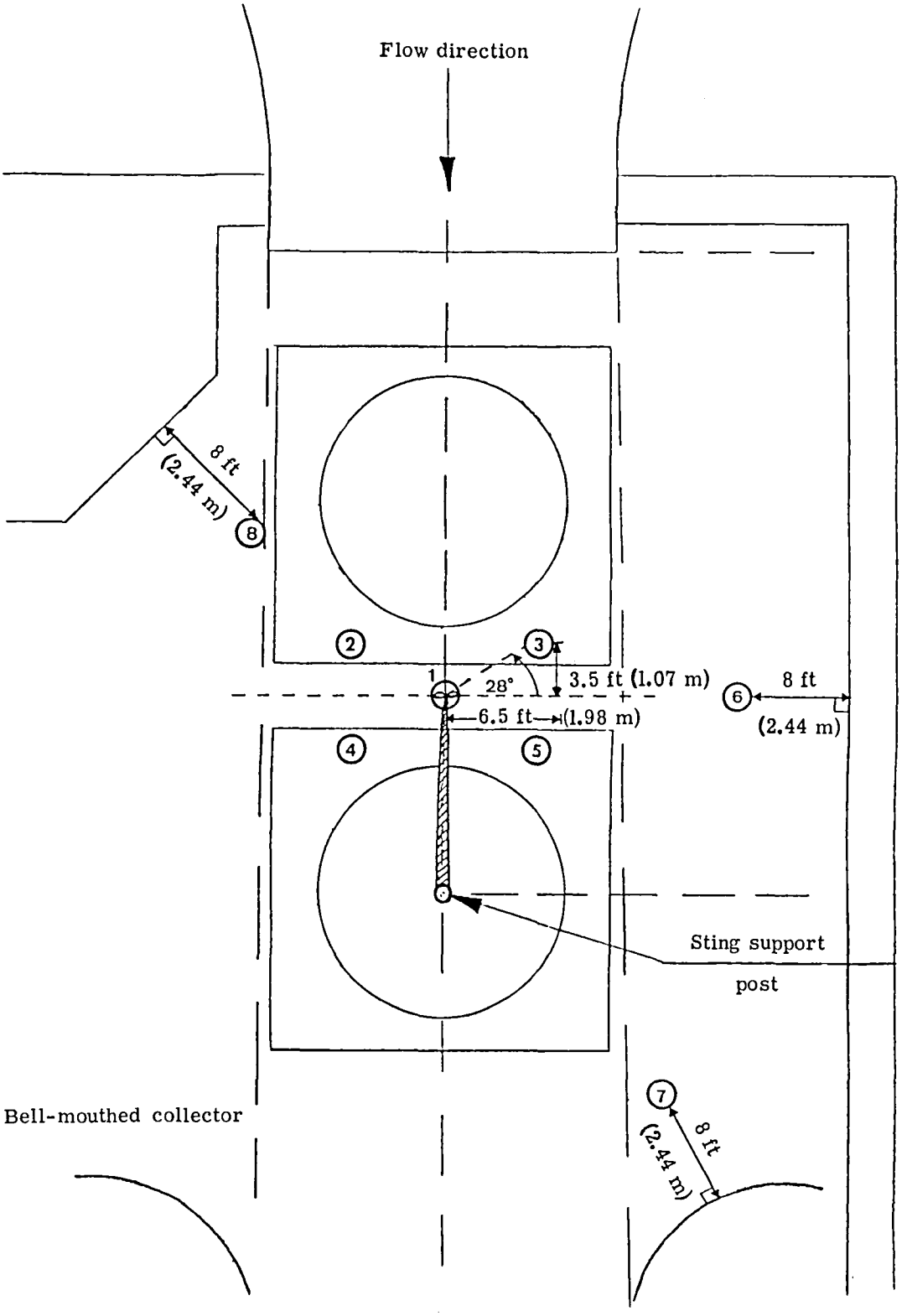

Figure 7. Sketch of microphone locations in open test section.

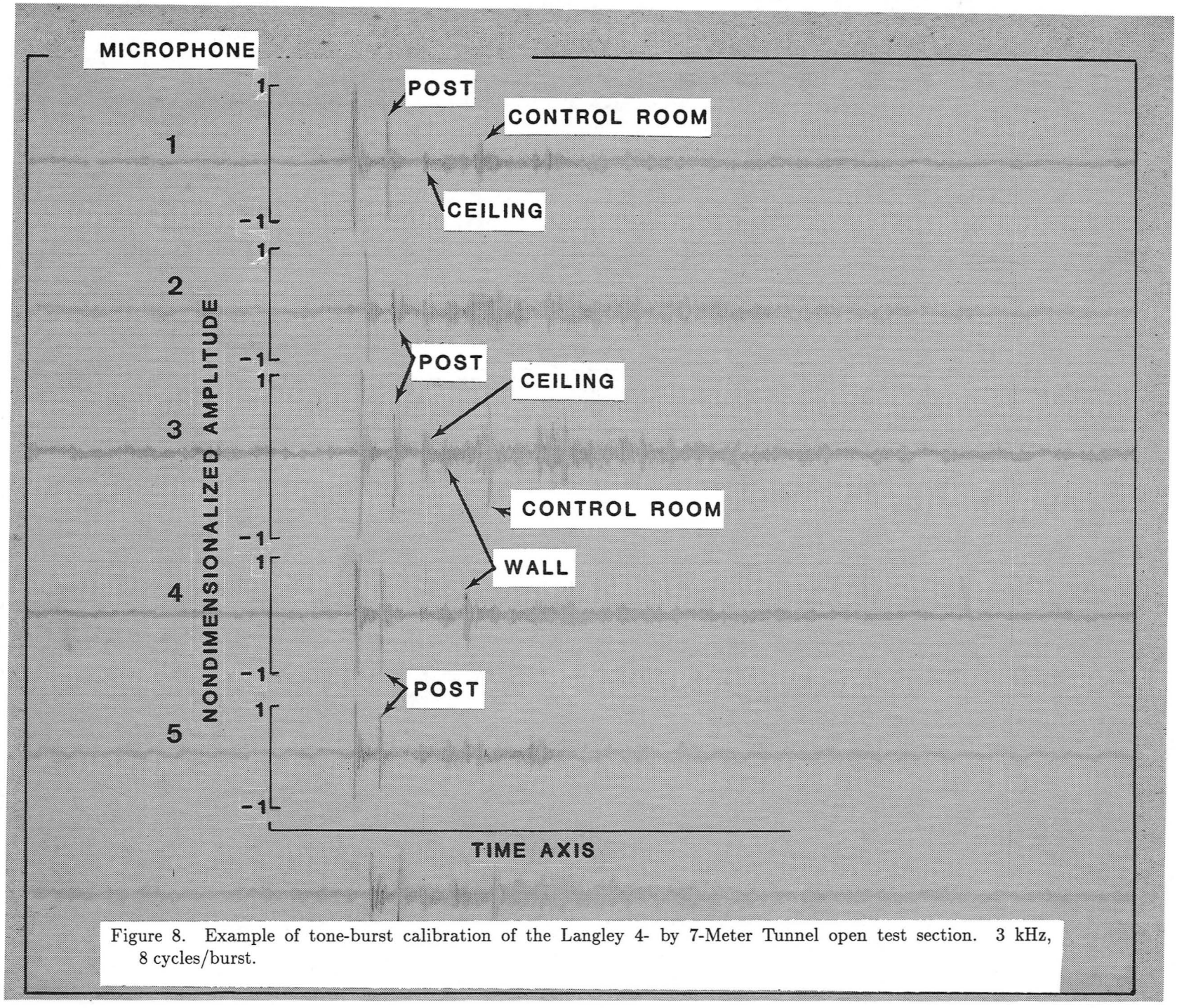

Figure 8. Example of tone-burst calibration of the Langley 4- by 7-Meter Tunnel open test section. 3 kHz, 8 cycles/burst.

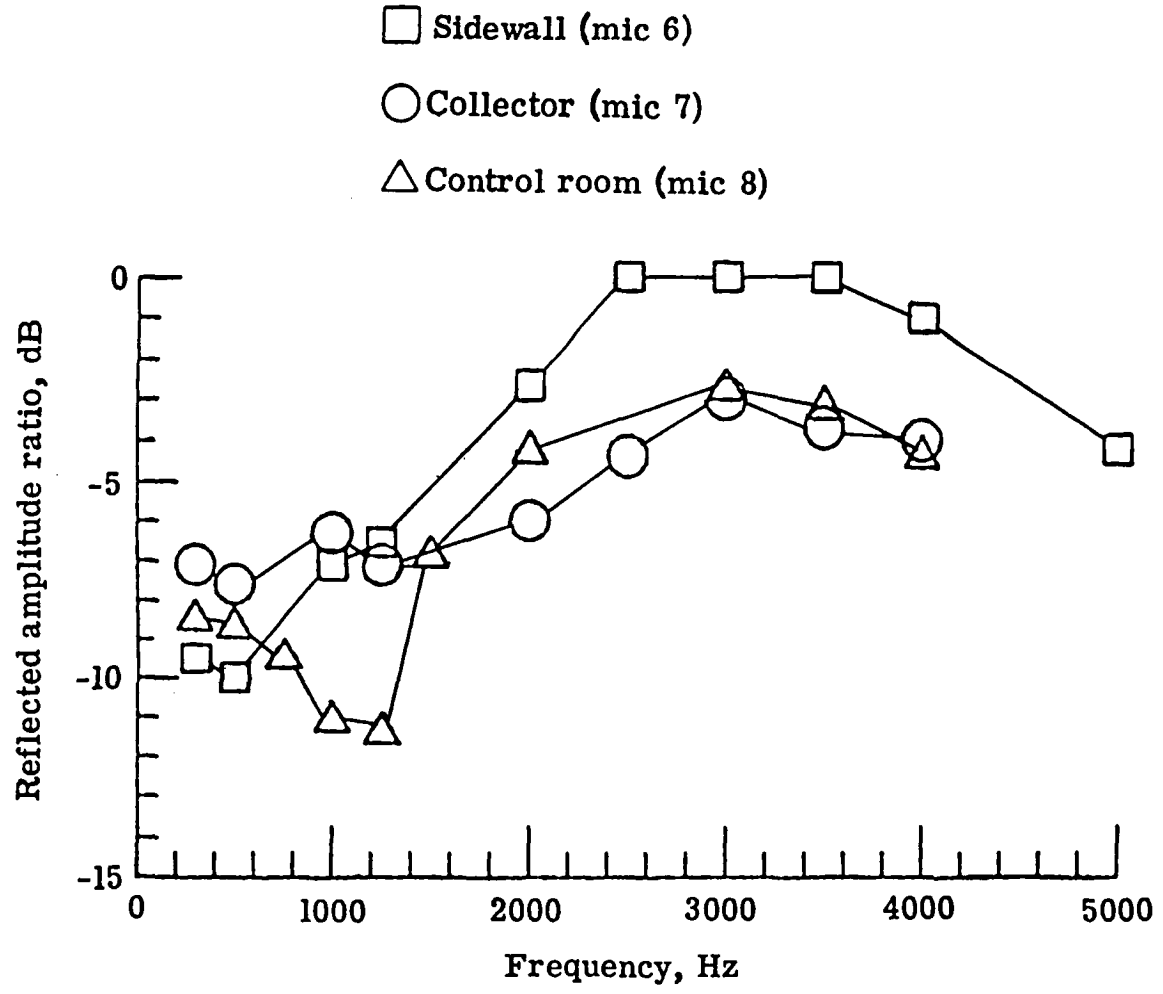

Figure 9. Reflection characteristics of open test section.

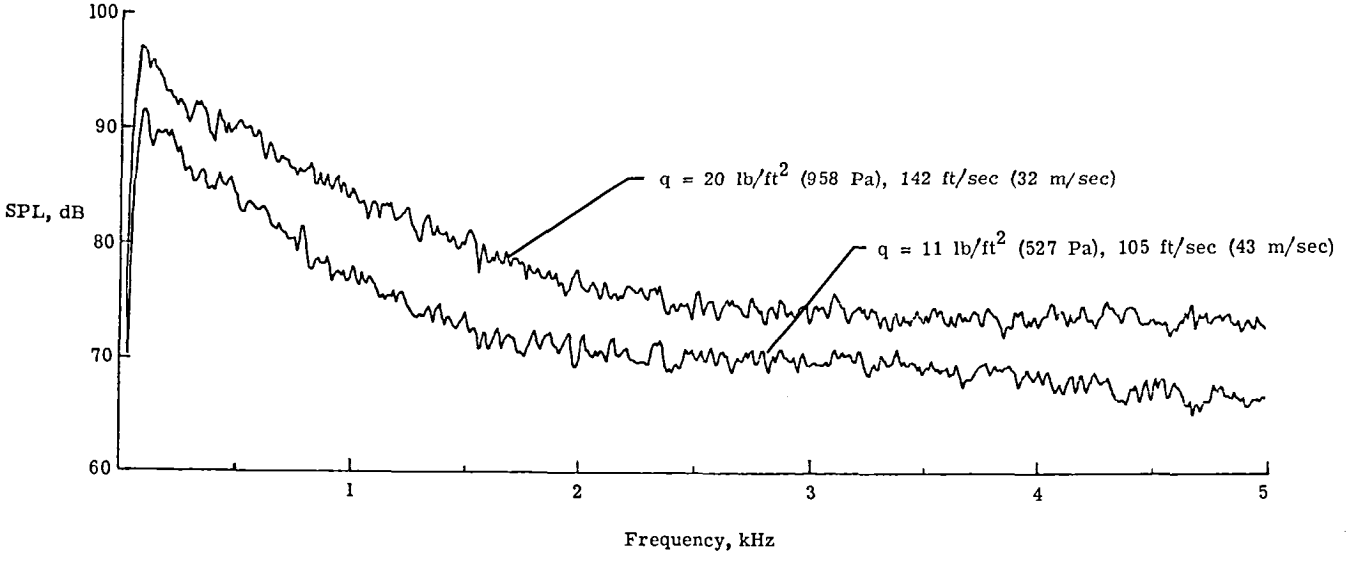

Figure 10. Narrow-band spectra of tunnel background noise at microphone 1. Analysis bandwidth = 19.5 Hz.

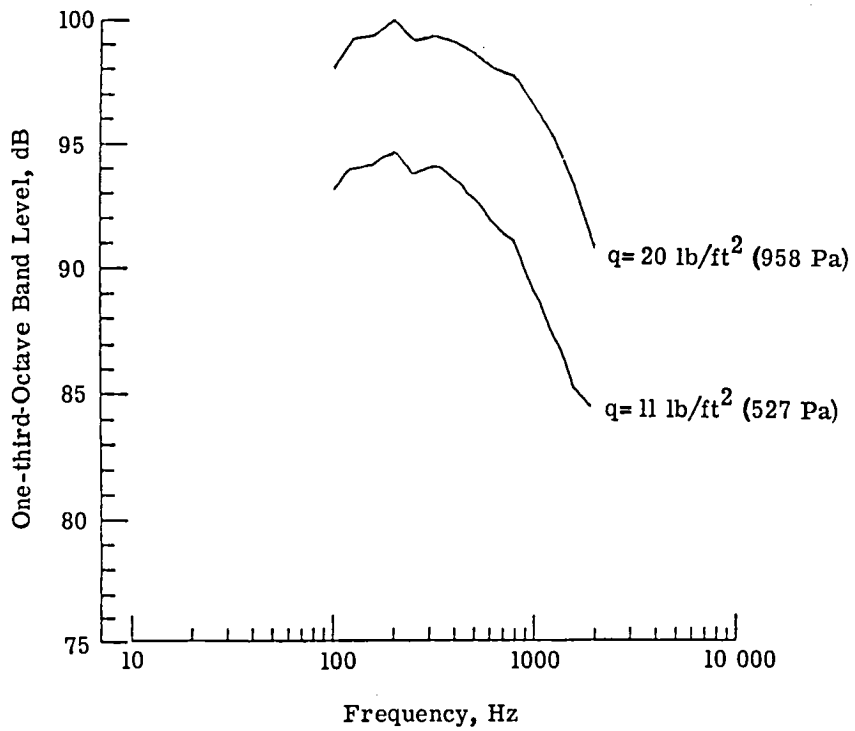

Figure 11. One-third-octave band background noise levels for microphone 1.

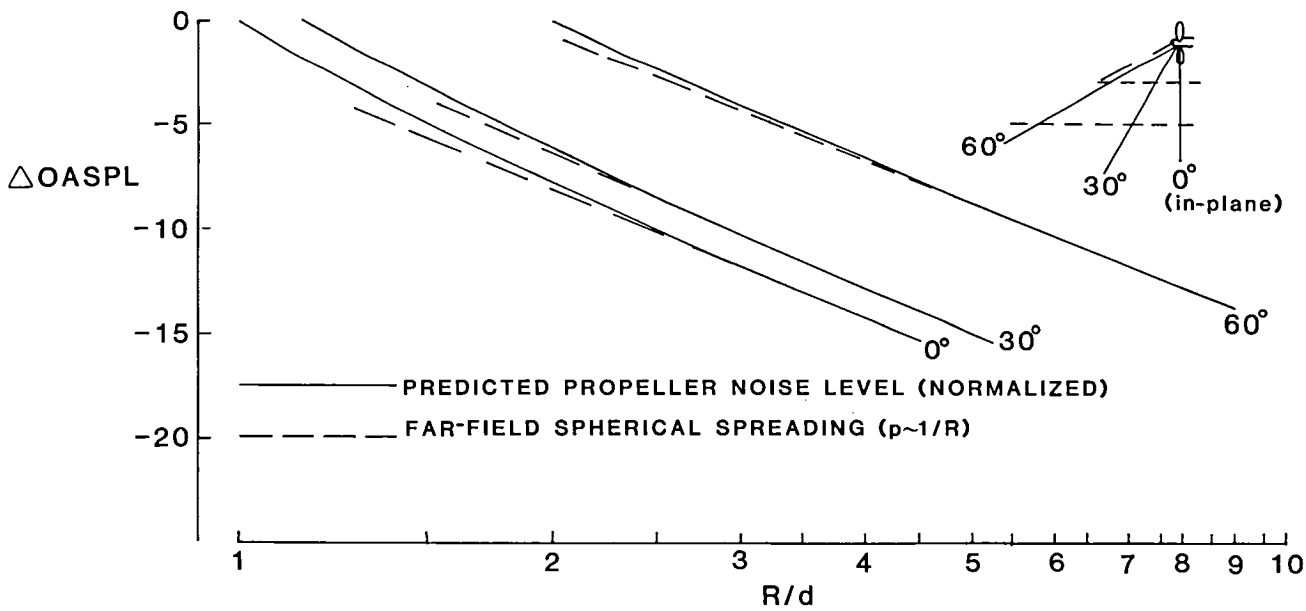

Figure 12. Predicted location of propeller far-field using spherical spreading law.

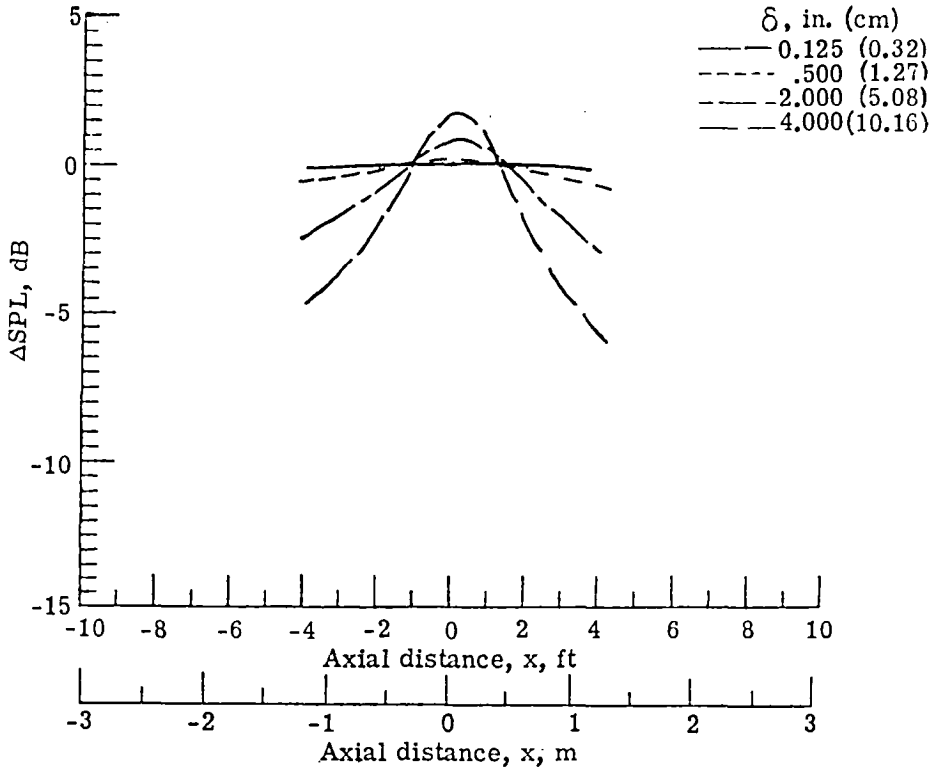

(a) First harmonic.

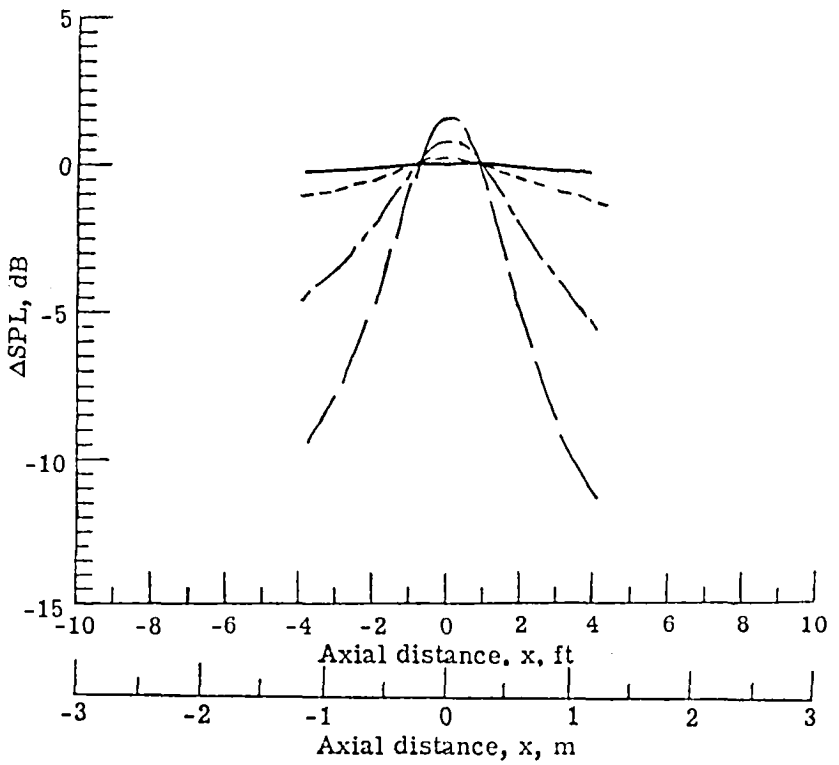

(b) Second harmonic.

Figure 13. Predicted effect of tunnel boundary layer.

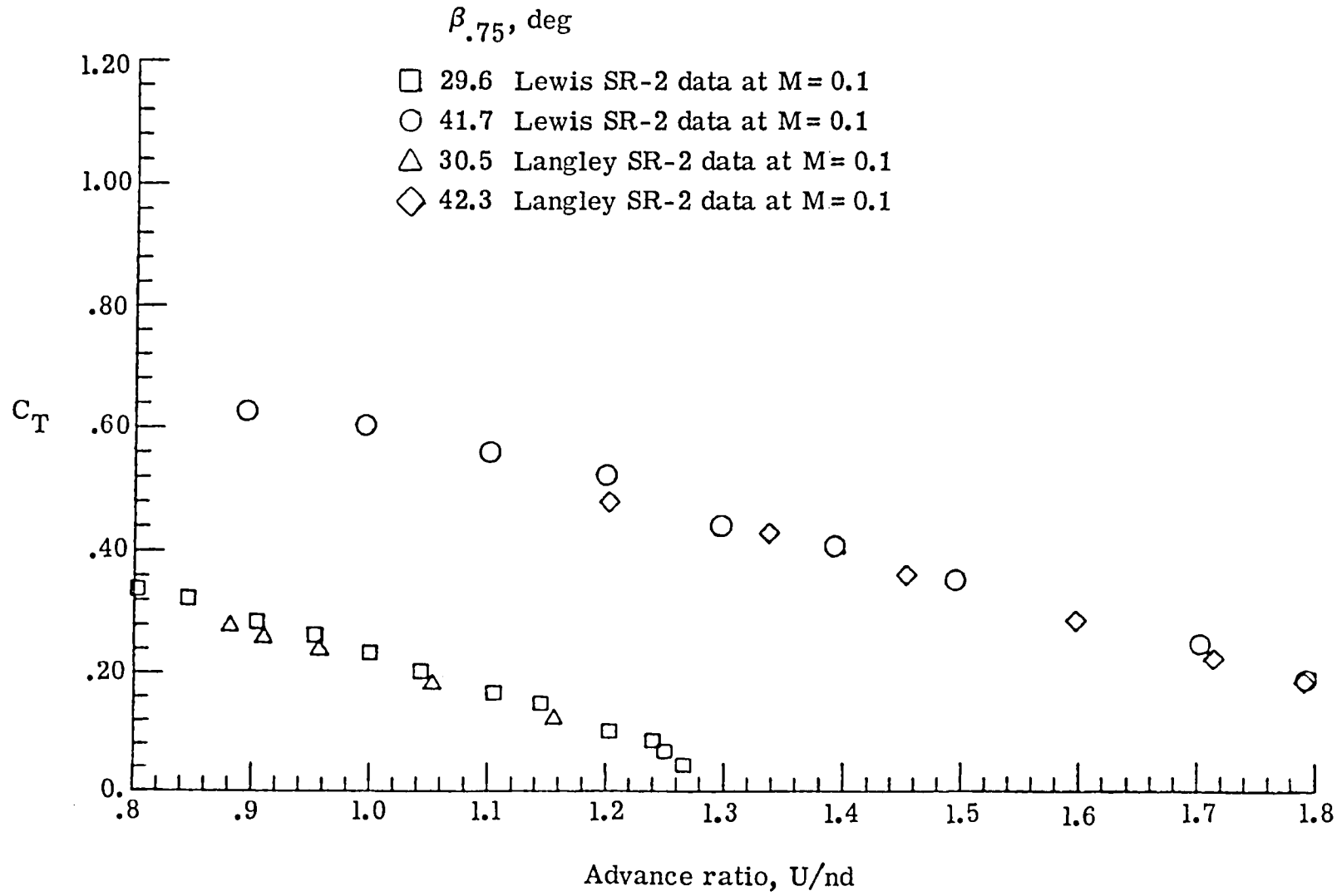

(a) Thrust coefficient.

Figure 14. Performance comparisons.

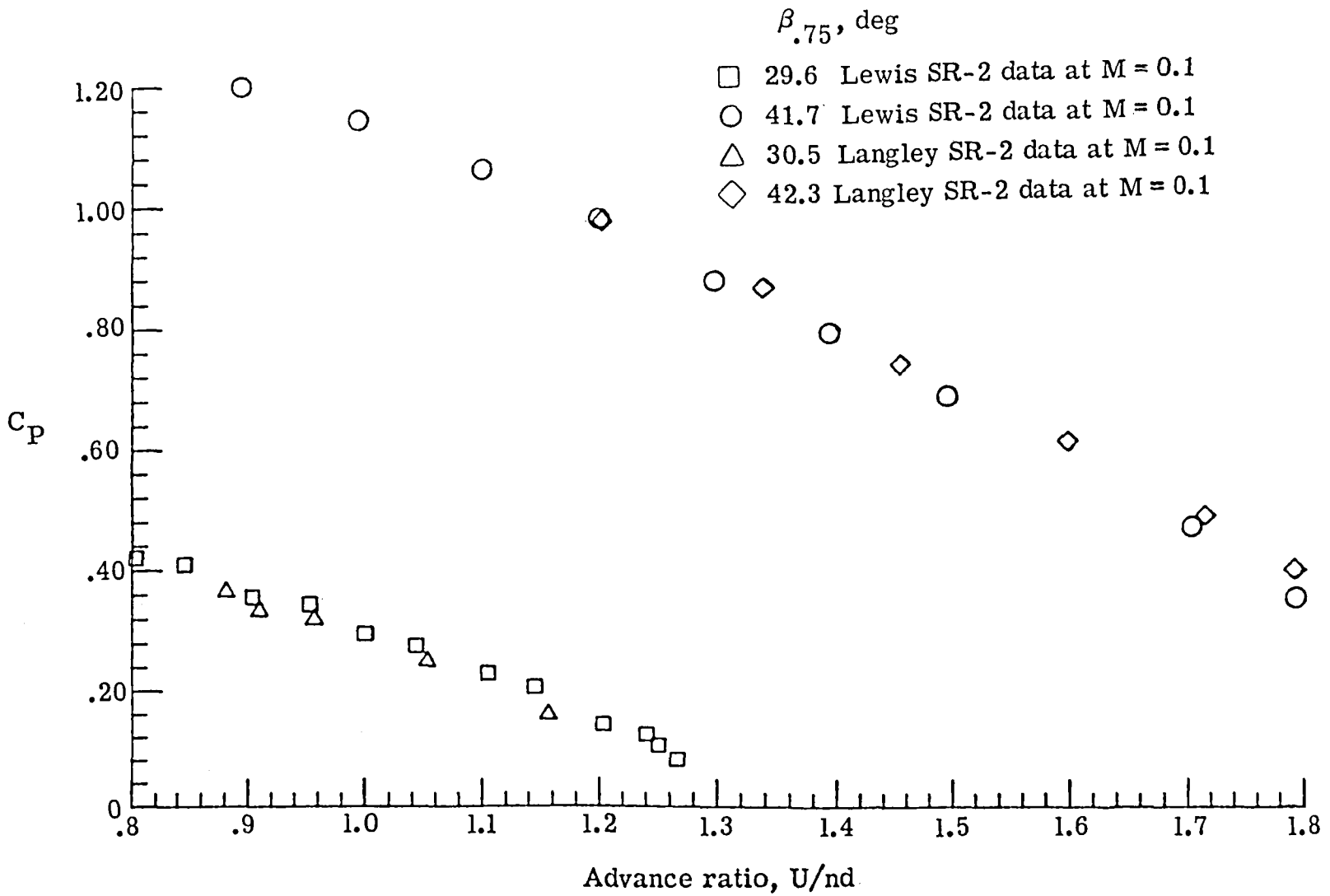

(b) Power coefficient.

Figure 14. Concluded.

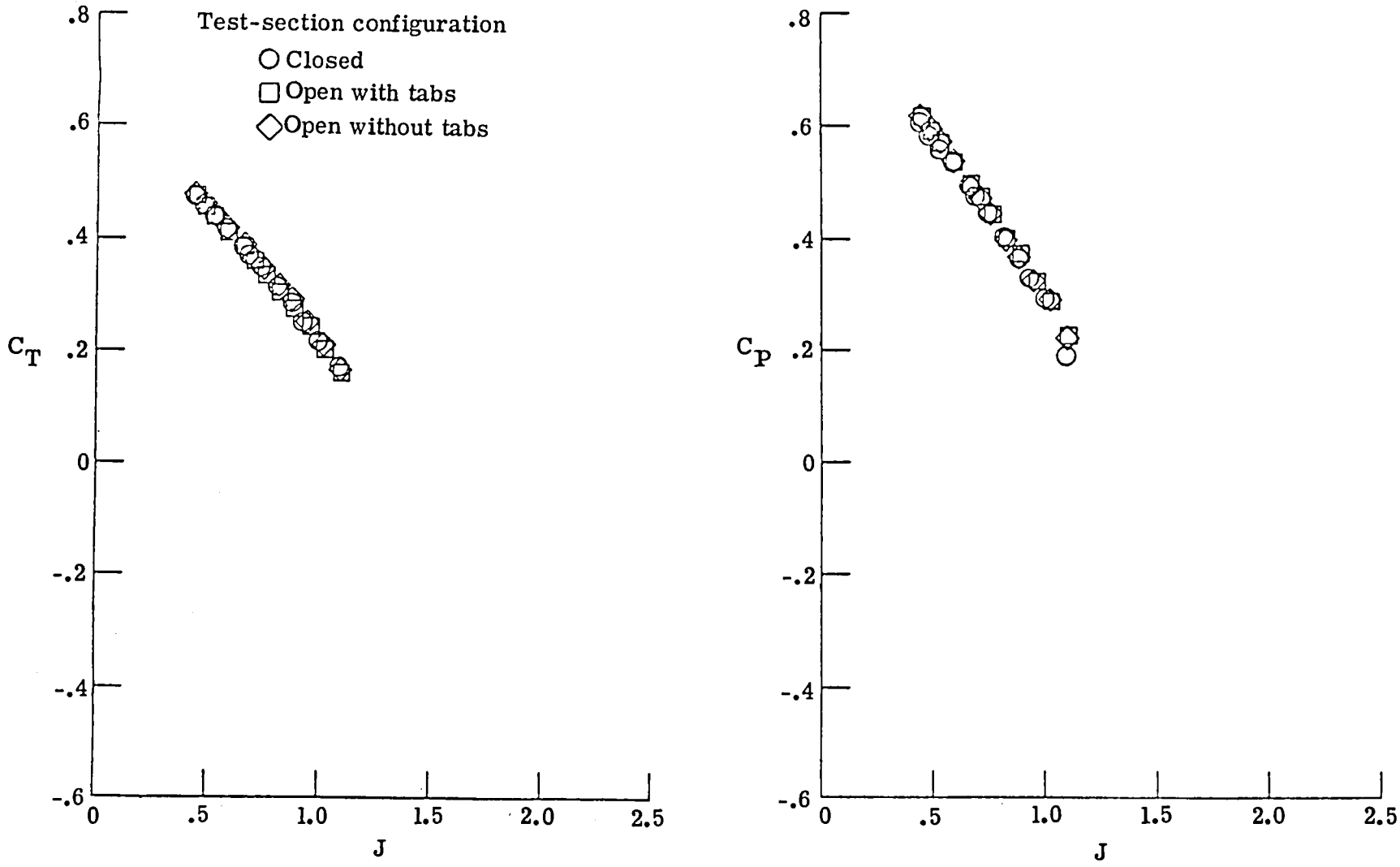

(a) $q = 4.5$ lb/ft^2 (215 Pa).

Figure 15. Effect of tunnel configuration on propeller performance. $\beta_{.75} = 30.5$.

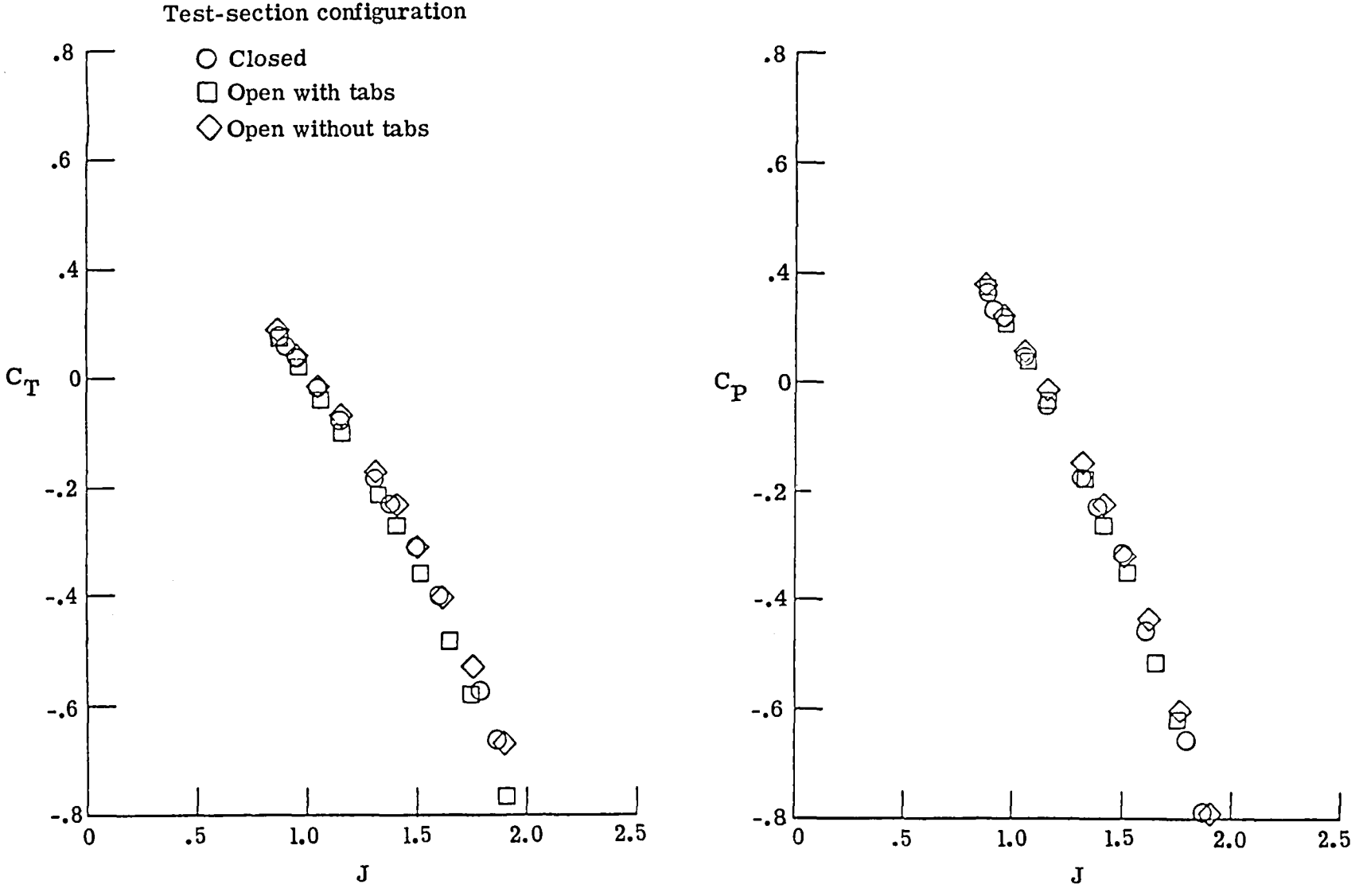

(b) $q = 18.0$ lb/ft^2 (862 Pa).

Figure 15. Continued.

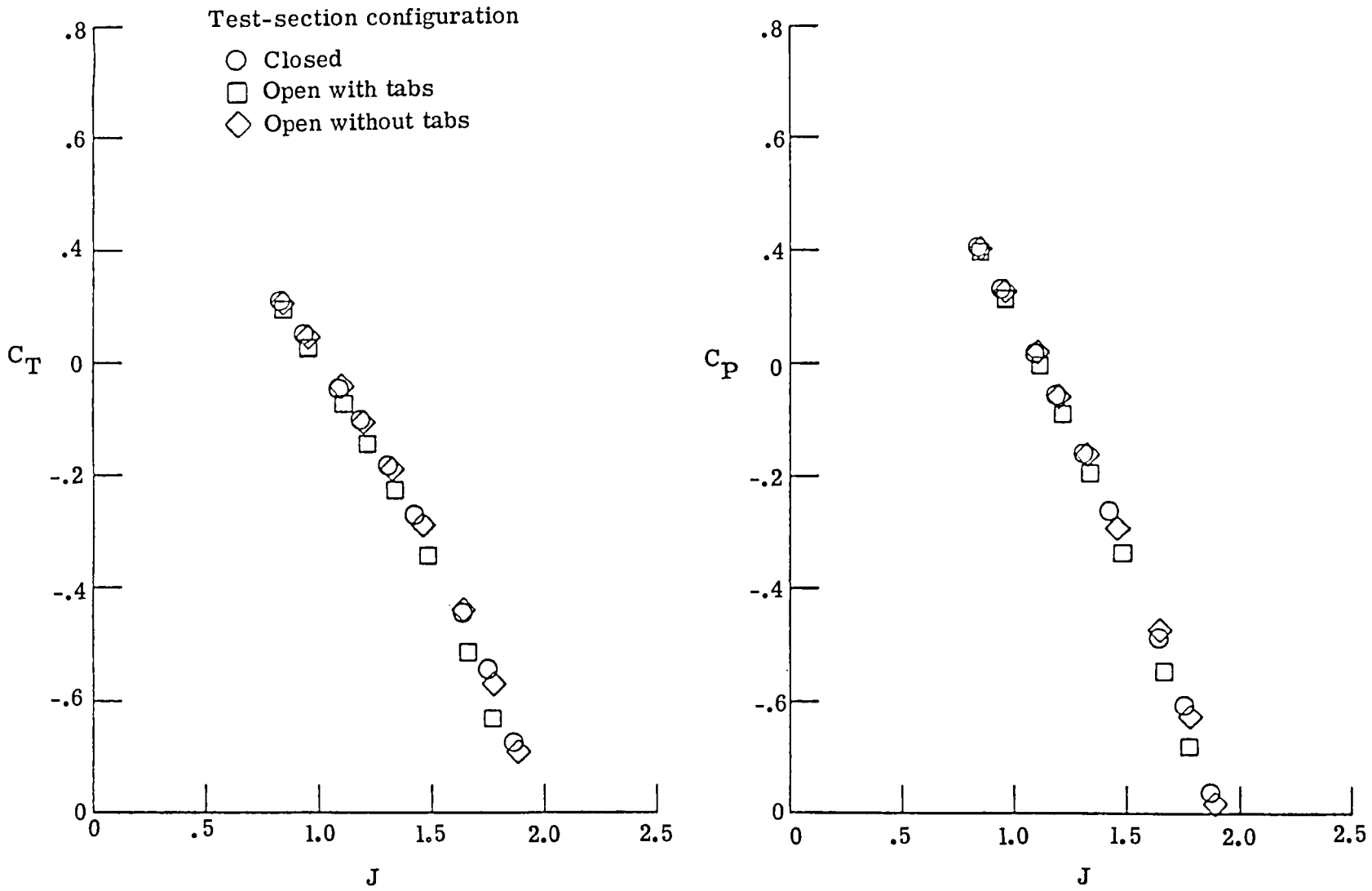

(c) 28.3 lb/ft^2 (1355 Pa).

Figure 15. Concluded.

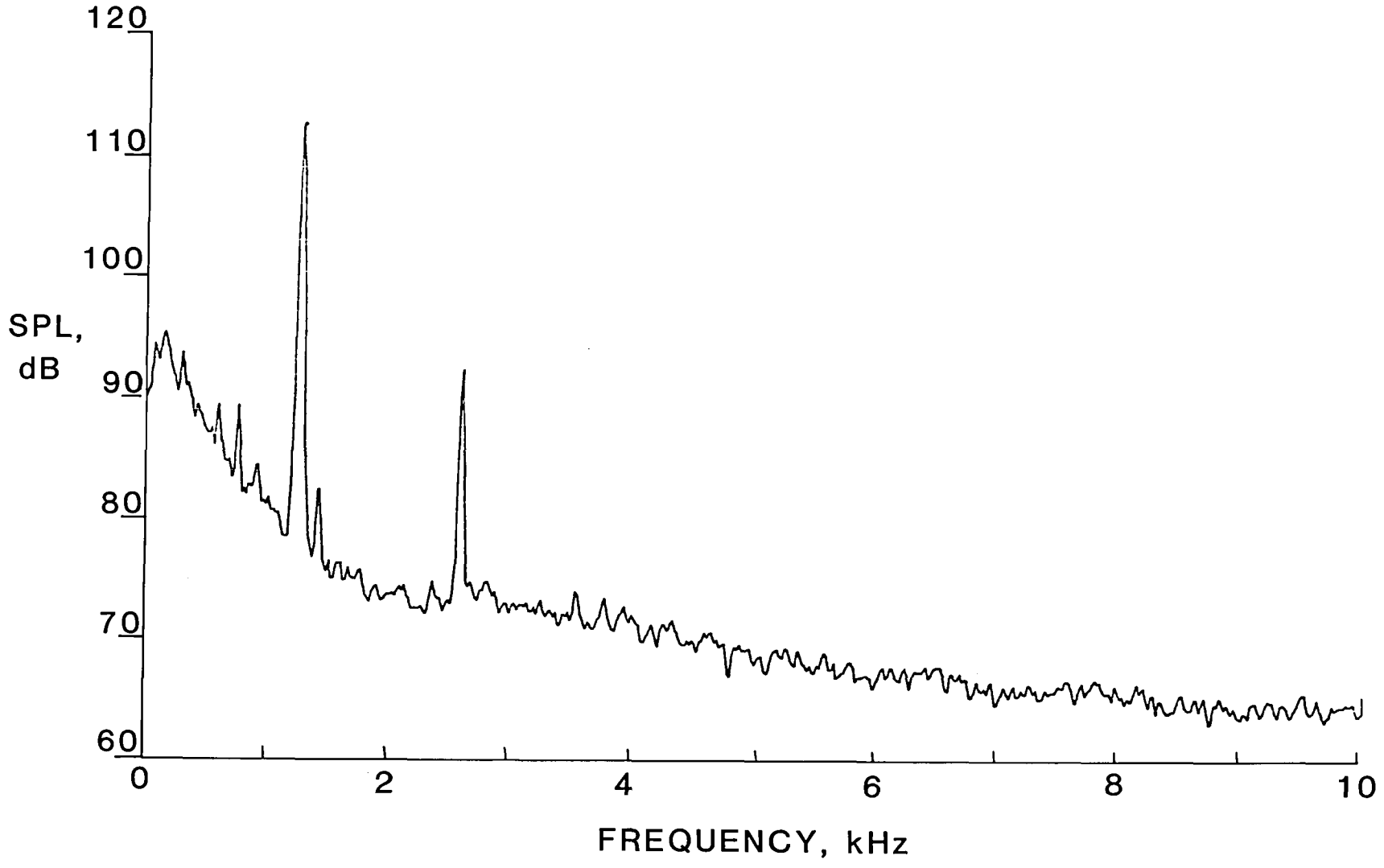

Figure 16. Typical narrow-band spectrum of SR-2 propeller noise measured at microphone 1. $\beta_{.75} = 20°$; $q = 11$ lb/ft^2 (527 Pa), $\alpha = 0°$ Data are not corrected for pressure doubling.

1. Report No.	2. Government Accession No.	3. Recipient's Catalog No.
NASA TM-85721		

4. Title and Subtitle	5. Report Date
EVALUATION OF THE LANGLEY 4- BY 7-METER TUNNEL FOR PROPELLER NOISE MEASUREMENTS	December 1984
	6. Performing Organization Code: 535-03-12-08
7. Author(s): P. J. W. Block and Garl L. Gentry, Jr.	8. Performing Organization Report No.: L-15738
9. Performing Organization Name and Address: NASA Langley Research Center, Hampton, VA 23665	10. Work Unit No.
	11. Contract or Grant No.
12. Sponsoring Agency Name and Address: National Aeronautics and Space Administration, Washington, DC 20546	13. Type of Report and Period Covered: Technical Memorandum
	14. Sponsoring Agency Code

15. Supplementary Notes

16. Abstract

An experimental and theoretical evaluation of the Langley 4- by 7- Meter Tunnel was conducted to determine its suitability for obtaining propeller noise data. This report describes the tunnel circuit and open test section. An experimental evaluation is performed using microphones placed in and on the tunnel floor. The reflection characteristics and background noise are determined. The predicted source (propeller) near-field/far-field boundary is given using a first-principles method. The effect of the tunnel-floor boundary layer on the noise from the propeller is also predicted. A propeller test stand used for part of this evaluation is also described. The measured propeller performance characteristics are compared with those obtained at a larger scale, and the effect of the test-section configuration on the propeller performance is examined. Finally, propeller noise measurements were obtained on an eight-bladed SR-2 propeller operating at angles of attack −8°, 0°, and 4.6° to give an indication of attainable signal-to-noise ratios.

17. Key Words (Suggested by Authors(s))	18. Distribution Statement
Wind tunnel Wind-tunnel noise Propeller noise Propeller performance Background noise	Unclassified—Unlimited Subject Category 71

19. Security Classif.(of this report)	20. Security Classif.(of this page)	21. No. of Pages	22. Price
Unclassified	Unclassified	28	A03

For sale by the National Technical Information Service, Springfield, Virginia 22161

NASA-Langley, 1984